Current-Based Diagnosis for Gear Tooth Breaks in Wind Turbine Gearboxes

Dingguo Lu
Student Member, IEEE
Department of Electrical Engineering
University of Nebraska-Lincoln
Lincoln, NE 68588-0511 USA
Stan1860@huskers.unl.edu

Xiang Gong
Student Member, IEEE
Department of Electrical Engineering
University of Nebraska-Lincoln
Lincoln, NE 68588-0511 USA
xiang.gong@huskers.unl.edu

Wei Qiao
Member, IEEE
Department of Electrical Engineering
University of Nebraska-Lincoln
Lincoln, NE 68588-0511 USA
wqiao@engr.unl.edu

Abstract—**Gearbox faults constitute a significant portion of all faults and downtime in wind turbines (WTs). Current-based gearbox fault diagnosis has significant advantages over traditional vibration-based techniques in terms of cost, implementation, and reliability. This paper derives a mathematical model for a WT drive train consisting of a two-stage gearbox and a permanent magnet (PM) generator, from which the characteristic frequencies of gear tooth breaks in generator stator current frequency spectra are clearly identified. A adaptive signal resampling algorithm is proposed to convert the variable fault characteristic frequencies to constant values for WTs running at variable speeds. A fault detector is proposed for diagnosis of gear tooth breaks using statistical analysis on the fault signatures extracted from the stator current spectra. Experimental results on a real gearbox are provided to show the effectiveness of the proposed model and method for diagnosis of gear tooth breaks.**

Keywords—**adaptive resampling, condition monitoring, current, fault diagnosis, gearbox, permanent magnet (PM) generator, tooth break, wind turbine (WT)**

I. INTRODUCTION

Gearbox is considered the most troublesome part in modern WTs [1]. Failure of a gearbox is likely to have a great impact on WT availability owing to a long time needed to remove the failed gearbox from the nacelle for repair or replacement [2]. The statistical analysis from the wind energy industry corroborates that gearbox failures share about 20% of the total downtime in WTs [3], which is the leading proportion among all the components. Hence, it is highly desired to detect gearbox faults at an early stage and repair the faulted gearbox in a timely manner to reduce downtime and prevent catastrophic damages of the WT.

WT condition monitoring and fault diagnosis techniques are still under development. Conventional fault diagnosis techniques require additional mechanical sensors and data acquisition devices to implement [4], [5]. These sensors and devices are inevitably subject to failure, which could cause additional problems to system reliability and additional operating and maintenance costs. Current-based (mechanical-sensorless) fault diagnosis techniques are promising alternatives [4], [6]–[8]. These techniques only use generator current measurements that are already used for monitoring, control, and protection of WTs; no additional sensors or data acquisition devices are needed. Moreover, current signals are reliable and easily accessible from the ground without intruding the WTs. Therefore, current-based fault diagnosis techniques have great operational and financial benefits and promising potential to be adopted by the wind energy industry.

This paper proposes a current-based method for diagnosis of gear tooth defects in WT gearboxes. A mathematical model is developed for an emulated WT drive-train system consisting of a two-stage gearbox and a PM wind generator to identify the characteristic frequencies of gear tooth breaks in the generator stator current signal. For WTs running at variable speed, the characteristic frequencies vary with the shafting rotating speed. An adaptive interpolation-based signal resampling algorithm is proposed to convert variable fault characteristic frequencies of the gearbox to constant values. A fault detector is then developed based on the statistical analysis of the sidebands around the fundamental and harmonics of the current signal to effectively detect the gear tooth break faults. Experimental studies are carried out on a gearbox driving a PM wind generator to validate the mathematical analysis and proposed method for gear tooth defect diagnosis.

II. CHARACTERISTIC FREQUENCIES OF A GEARBOX WITH GEAR TOOTH BREAKS

In a PM generator, the torsional vibration introduced on the shaft will cause magnetic field anomaly of the PM machine and, therefore, change the mutual and self-inductances of the machine, causing sidebands across current frequencies [9]. Meanwhile, the difference of the torsional vibrations between healthy and faulty cases of a
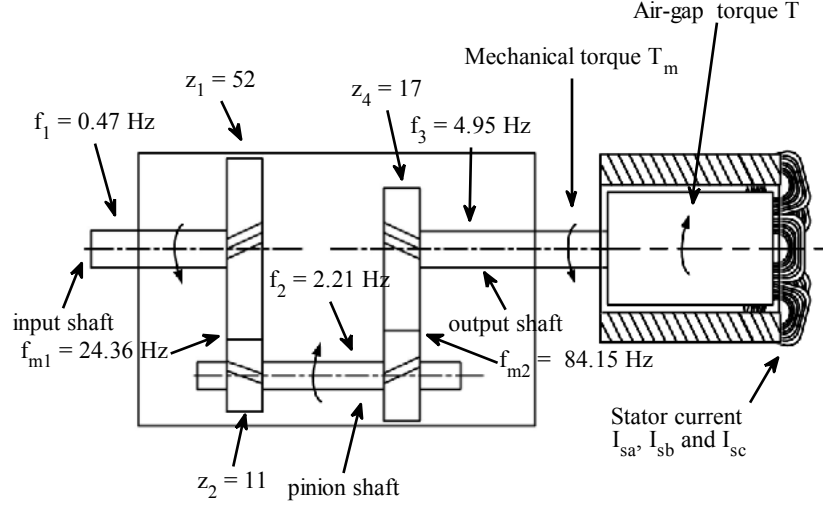
Fig. 1. Schematic of a two-stage gearbox connected to a PM machine with characteristic vibration frequencies.

gearbox will lead to variations in the rotating speed and shaft torque of the gearbox, which subsequently will cause changes in air-gap torque and the sidebands across the fundamental and harmonics of stator currents of a generator to which the gearbox is connected.

In this study a system consisting of a two-stage gearbox connected with a PM machine is considered, as shown in Fig. 1. The characteristics frequencies of gearbox vibration include the input shaft frequency f_1, pinion shaft frequency f_2, the output shaft frequency f_3, and various gear meshing frequencies f_{m1} and f_{m2}, where $z_1 - z_4$ are the tooth numbers of the four gears in the gearbox. Yacamini's research [10] has revealed that a single-frequency torsional vibration in a gearbox will affect the stator current of an electric machine connected to the gearbox and bring in sidebands in the current.

At a constant load condition, the air-gap torque of the PM machine consists of a constant component and some oscillatory components due to torsional vibrations at the frequencies of f_1, f_2, and f_3 with respective phases of $\emptyset_1$, $\emptyset_2$, and $\emptyset_3$, given by

$$T = T_0 + T_1 \cos(2\pi f_1 t + \phi_1) + T_2 \cos(2\pi f_2 t + \phi_2) + T_3 \cos(2\pi f_3 t + \phi_3) \tag{1}$$

Due to the torsional vibrations induced by transmission errors in the input, pinion, and output wheels and the stiffness variation of the gear teeth contact, the gearbox adds rotational and meshing frequency components into the torque signature of the output shaft [8]. It has also been inferred that high-frequency torsional vibrations are being damped by the mechanical components [10]. Therefore, only the effects of torsional vibrations caused by rotating frequencies of the shafts are considered in this article while deriving the resultant phase current expression.

Each stator phase current consists of two components: a magnetizing current component I_{SM}, which is zero when the

PM machine is running at unity power factor or I_{SM0} when the power factor is not unity, and a torque producing component I_{sT}, which is 90° ahead of the flux vector. The torque producing component has an average value of I_{sT0}. When torsional vibrations exist, the torque producing component is expressed as follows.

$$I_{sT} = I_{sT0} + A_{sT1} \cos(2\pi f_1 t + \phi_{T1}) + A_{sT2} \cos(2\pi f_2 t + \phi_{T2}) + A_{sT3} \cos(2\pi f_3 t + \phi_{T3}) \tag{2}$$

where $A_{sTi}(i = 1, 2, 3)$ represents the magnitude of each current component.

The current in any phase of the stator windings should contain sinusoidal fundamental frequency components plus its harmonics, if there is no vibration. With the existence of torsional vibrations, the stator current will be modulated by these vibrations. For example, the A-phase current can then be written as:

$$\begin{aligned} I_{sa} &= I_{sM} \sin 2\pi f_s t + I_{sT} \cos 2\pi f_s t \\ &= I_{sM0} \sin 2\pi f_s t T_0 + [I_{sT0} + A_{sT1} \cos(2\pi f_1 t + \phi_{T1}) \\ &\quad + A_{sT2} \cos(2\pi f_2 t + \phi_{T2}) \\ &\quad + A_{sT3} \cos(2\pi f_3 t + \phi_{T3})] \cos 2\pi f_s t \end{aligned} \tag{3}$$

where f_s is the fundamental frequency of the stator current. Simplifying the above equation gives, $I_{sa} = I_{sM} \sin 2\pi f_s t + I_{sT} \cos 2\pi f_s t$

$$\begin{aligned} &= I_0 + \frac{1}{2} A_{sT1}[\cos(2\pi(f_s - f_1)t - \phi_{T1}) + \cos(2\pi(f_s + f_1)t + \phi_{T1})] \\ &\quad + \frac{1}{2} A_{sT2}[\cos(2\pi(f_s - f_2)t - \phi_{T2}) + \cos(2\pi(f_s + f_2)t + \phi_{T2})] \\ &\quad + \frac{1}{2} A_{sT3}[\cos(2\pi(f_s - f_3)t - \phi_{T3}) + \cos(2\pi(f_s + f_3)t + \phi_{T3})] \end{aligned} \tag{4}$$

where $I_0 = \sqrt{I_{sM0}^2 + I_{sT0}^2}$.

Equation (4) indicates clearly that the torsional vibrations with specific frequencies will have sidebands across the electrical line frequencies in the PM machine stator current signature. Here only the fundamental component of the current is considered. In fact, these sidebands will also appear around harmonics, which can be derived in a similar way.

III. ADAPTIVE SIGNAL RESAMPLING

The characteristic frequencies of gearbox faults in a stator current signal are related to the gearbox shaft rotating frequency, and become nonstationary when the shafting rotating speed varies with time. It is difficult to extract the fault signatures from the nonstationary stator current signal of the PM machine using conventional spectrum analysis methods. In this case, the frequency spectrum generated by the classical Fast Fourier transform (FFT) is nonstationary and thus cannot be directly used for fault detection. However, if the gearbox runs at a constant speed, the classical FFT analysis should be able to generate stationary frequency spectrum of the stator current signal. In other words, if the characteristic frequencies of a gearbox fault are converted to constant values, the classical FFT analysis can then be used to detect the fault for a gearbox running at variable speeds.

Define Ω_r the normalized frequency of the shaft rotating frequency f_r in the gearbox, and f_{SF} the sampling frequency of the stator current samples. The relationship among Ω_r, f_r and f_{SF} is as following [11],

$$\frac{\Omega_r(t)}{2\pi} = \frac{f_r(t)}{f_{SF}} \qquad (5)$$

The sampling frequency f_{SF} is usually fixed at a specific value during data acquisition. This makes the normalized frequency vary with time if f_r is nonstationary. In this paper, Ω_r is expected to be constant to facilitate fault diagnosis. Hence, if f_{SF} is changed continuously according to f_r, Ω_r will be constant subsequently. This paper proposed an adaptive signal resampling algorithm to convert the current samples from a fixed sampling frequency to an adaptive sampling frequency to make Ω_r constant, which is shown in Fig. 2 and implemented in the following steps.

(1) Sample the measured nonstationary generator stator current with a fixed sampling rate, and the result is $C(n)$, where $n = 1, 2, 3, \dots, N$ and N is the length of the stator current samples.

(2) Calculate the instantaneous amplitude of the current samples by using Hilbert transform to normalize the stator current samples [12], and the result is $S(n)$.

(3) Estimate the rotating frequency $f_r(n)$ of the gearbox output shaft based on the normalized current samples $S(n)$ by using a phase-locked loop (PLL) method.

(4) Let $i = 0$ and define $L_i(n)$ the initial location of the normalized current sample $S(n)$, where i represents the order of interpolation.

(5) Let $i = i + 1$ and calculate the location $L_i(n)$ of each normalized sample $S(n)$ as follows.

$L_i(1) = 1;$

$$L_i(n) = L_i(n-1) + \frac{(N-1) \cdot [f_r(n) + f_r(n-1)]^{-1}}{\sum\limits_{m=2}^{M} [f_r(m) + f_r(m-1)]^{-1}}$$

for $n \geq 2$.

(6) Interpolate the samples $S(n)$ using the Cubic spline interpolation method based on their new locations $L_i(n)$, and the result is $S_{re}(n)$.

(7) Repeat Steps (5) and (6) until $\sum_{n=1}^{N} |L_{i+1}(n) - L_i(n)|$ is smaller than a predetermined threshold C_r. This means that the last two sequential sets of locations are sufficiently close and, hence, no significant interpolation can be made for the samples by using one more iteration. Therefore, the iteration stops.

(8) Choose a base frequency f_b, to which the fundamental frequency of the processed current samples will be converted.

(9) Perform frequency spectrum analysis.

By using the proposed algorithm, the variable characteristic frequencies of the gearbox can be converted to constant values in the frequency spectrum of $S_{re}(n)$. The resulting frequency spectrum can then be used as signatures to clearly evaluate the condition of the gearbox.

IV. FAULT DETECTOR

A fault detector using statistical analysis on stator current signatures is proposed. For the six frequency components (i.e., the sidebands) in (4) cross a specific harmonic, the magnitude of each frequency component, M_i ($i = 1 \cdots 6$), is first normalized using (6). Then the mean value of each frequency component pair $f_s \pm f_i$ is calculated for both the healthy case and tooth break case by (7).

$$M_i' = \frac{M_i}{\sum M_i / 6} \qquad (6)$$

$$M = \frac{1}{2}(M'_{fs-fi} + M'_{fs+fi}) \qquad (7)$$

$$NPD_j = M_{fault} - M_{health} \qquad (8)$$

An evaluation matric called the normalized power difference NPD_j, $(j = 1, 2, 3)$, between the healthy case and

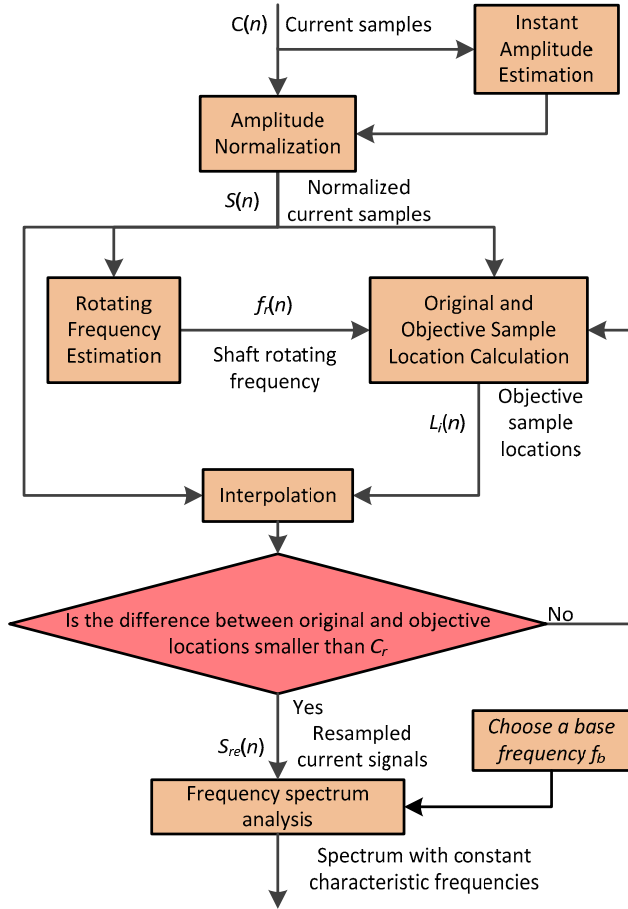tooth break case is defined in (8) and can be utilized to detect the gearbox fault.

Fig. 2. Schematic of the adaptive signal resampling algorithm.

V. EXPERIMENTAL RESULTS

Fig. 3 shows the experimental system setup. The system consists of a 300-W EXTRACTOR WT PM generator driven by a variable-speed induction motor through two back-to-back connected SIEMENS gearboxes, which are two-stage helical gearboxes with a total gear ratio of 10.57.

One gearbox (i.e., the speed reducer) reduces the shaft speed of the induction motor, which is driven by an adjustable-speed AC drive. The induction motor drive and

speed reducer are used to emulate the dynamics of a wind turbine rotor. The second gearbox, i.e., the testing gearbox, is used to emulate the gearbox in a WT. The testing gear is mounted at the input shaft of the testing gearbox and pretreated by removing one gear tooth, as shown in Fig. 4. By mounting the WT on the foundation through a single pole, the test bed is specially designed to simulate a real WT running under harsh conditions in nature environment. The system is firstly tested for constant-speed conditions and then variable-speed conditions controlled by the AC drive. One phase stator current of the PM generator is recorded via a Fluke current clamp and National Instrument (NI) data acquisition system with a sampling rate of 10 kHz. The current samples are acquired by the NI LabView installed in a laboratory computer. The length of the data record is 210 s.

Fig. 4. The testing gear with one tooth removed.

Frequency spectra, which are generated by FFT, of the stator currents for the gearbox with a healthy gear and a faulty gear are shown in Fig. 5, when the PM generator is running at a constant speed of 297 RPM. As shown in Fig. 5(a), the fundamental component of the stator current and its sidebands are observed in the healthy gear case. Meanwhile, same frequency components can be observed in Fig. 5(b) for the tooth break case. The observation verifies the theoretical derivation of the characteristic frequencies in Section II.

By comparing Figs. 5(a) and (b), it can be discovered that the gear tooth break fault has altered the sideband distribution. Further analysis is carried out by using the proposed fault detector. Fig. 6 shows the NPD of $f_s \pm f_2$ is less than zero while the NPD of $f_s \pm f_3$ is larger than zero, which means that the gear tooth break reduces the normalized power of $f_s \pm f_2$ while increasing the
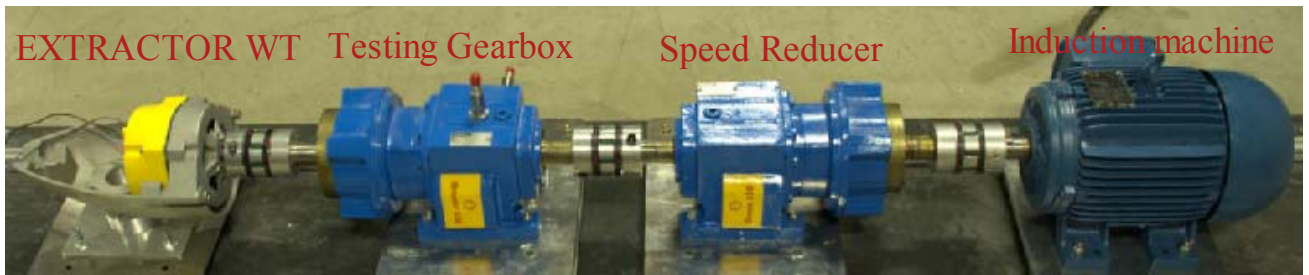

Fig. 3. The experimental system.

normalized power of $f_s \pm f_3$. The sideband distribution around the fundamental therefore has been affected by the torsional vibrations in the gearbox and the NPDs demonstrate a V shape. Similar phenomena can be found around the 5th and 7th harmonics of the stator current. Hence, the changes in the NPDs of the sidebands can be used as an operative index for effective detection of the tooth break fault. This is called a "V-shape" fault detector.

Same comparisons on the NPDs of the stator current are carried out for the PM generator operating at 297 RPM with 2% load and 891 RPM with 10% load, as shown in Figs. 7 and 8. Similar conclusion to that of Fig. 6 can be made. Since the NPDs are generated with normalized power of the stator current, the effects of different load conditions and speeds are eliminated. The results have proved that the proposed method, "V-shape" fault detector, is effective in detecting gear tooth breaks in the gearbox for different operating conditions.
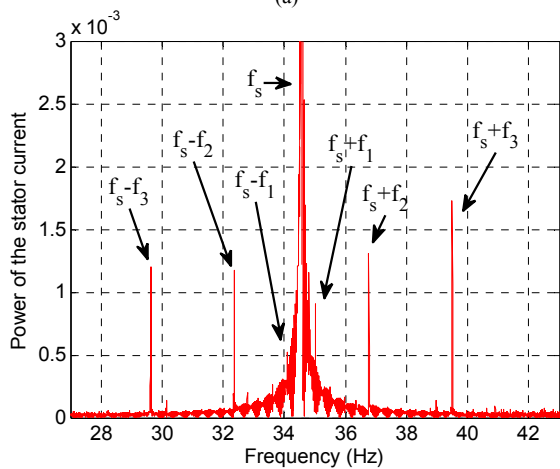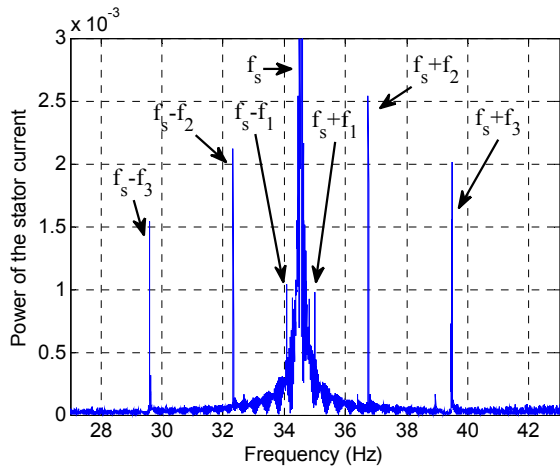
Fig. 6. Comparison of NPDs at 10% load and 297 RPM of the PM machine.

Fig. 5. Fundamental component of the stator current and its sidebands: (a) healthy gear case, (b) tooth break case.
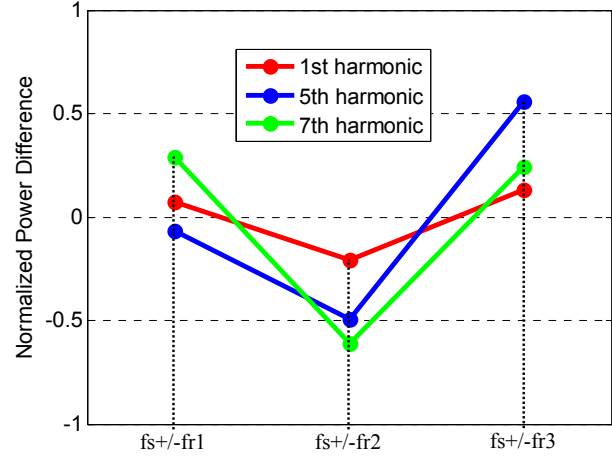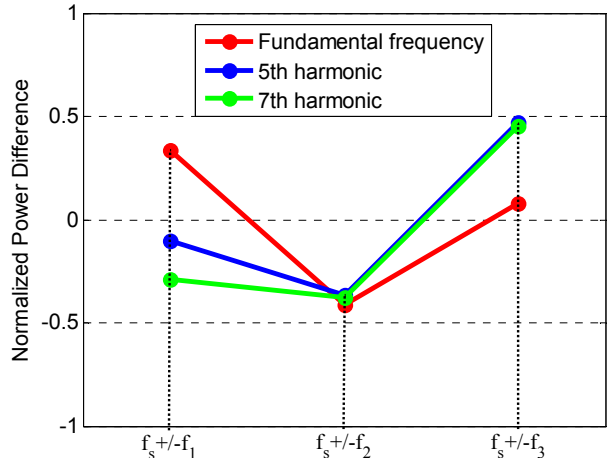
Fig. 7. Comparison of NPDs at 2% load and 297 RPM of the PM machine.
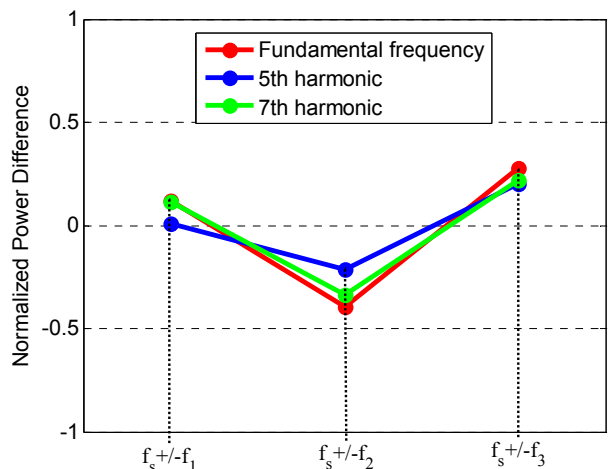
Fig. 8. Comparison of NPDs at 10% load and 891 RPM of the PM machine.

The proposed technique is also tested on the system at variable-speed conditions, where the speed of PM machine

input shaft (output shaft of the gearbox) is randomly varied within the range of 297 to 891 RPM. Each speed condition lasts for 8 seconds. The period of 8 seconds is chosen to simulate the wind speed in the natural environment.

If conventional FFT technique is directly applied to the recorded stator current samples, the resulting frequency spectrum is shown in Fig. 9. It can be seen that there are no specific characteristic frequencies of the gearbox observable in the frequency spectrum. It means that the classical FFT analysis fails to extract the fault signatures from the stator current signal.

The proposed adaptive signal resampling algorithm is then applied to perform signal conditioning to facilitate diagnosis of the tooth break faults under variable-speed conditions. During the execution of the algorithm, the PLL method is firstly used to estimate the shaft rotating speed of the PM machine, as shown in Fig. 10. Subsequently, the original and objective sample locations are calculated based on the estimated speed and the interpolation process is implemented, as described in Section III. Totally 16 interpolations have been implemented. A base frequency of 291 RPM is chosen for the purpose of comparing with certain constant-speed case at 291 RPM. The base frequency can also be other frequencies alternatively, as along as corresponding constant-speed baseline cases are available for comparison. After signal resampling, classical FFT method is used to generate the frequency spectrum from the resampled stator current signal, as shown in Fig. 11.

The characteristic frequencies of the gearbox, predicted by mathematical mode in Sec. II, can then be observed, including the fundamental frequency of the stator current and sidebands across it. The distribution of these sidebands is similar to those of constant-speed case in Fig. 5. Although the frequency components are interfered by noise, it can still be concluded that the proposed method successfully converts the variable-speed condition to a constant-speed condition and extracts the current signatures for fault diagnosis.

It should be noticed that the magnitude of each frequency component in Fig. 11 is greatly different from that in Fig. 5. This is caused by the amplitude normalization in the process of resampling. The power of the stator current here is so-called "normalized", holding different meaning. The proposed method studies the trend how sideband distribution changes and the absolute value of the frequency component magnitude will be normalized in the proposed fault detection. The impacts of different load conditions and speeds are eliminated with the normalized power of the stator current. Therefore, the effect of fault detector will not be influenced,

The proposed fault detector is then applied on the frequency spectrum and the result is shown in Fig. 12. Similar phenomenon as constant-speed conditions can be observed for the variable-speed condition. A "V-shape" fault detector reveals the NPD for different harmonics of the stator current.
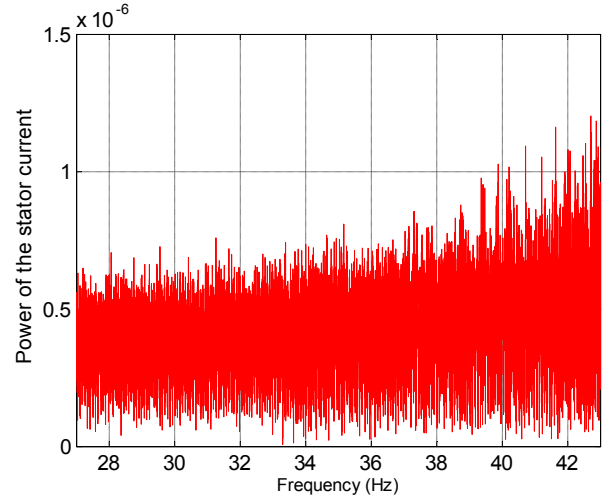

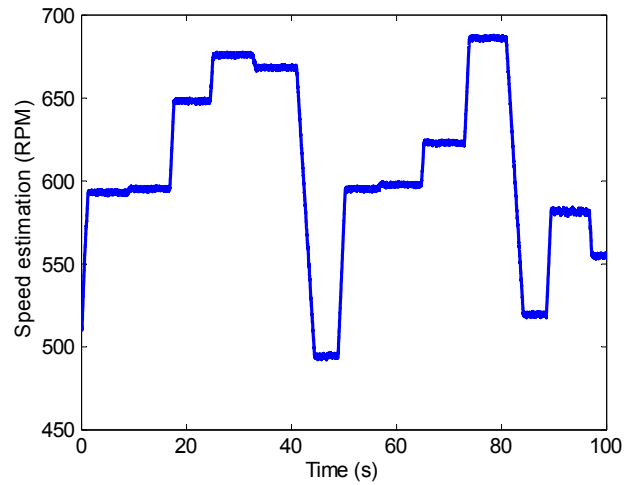Fig. 9. Frequency spectrum obtained from classical FFT analysis.

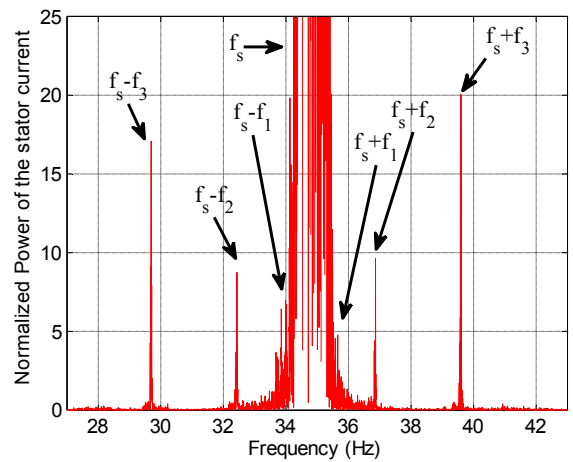Fig. 10. Shaft rotating speed estimated by the PLL method.

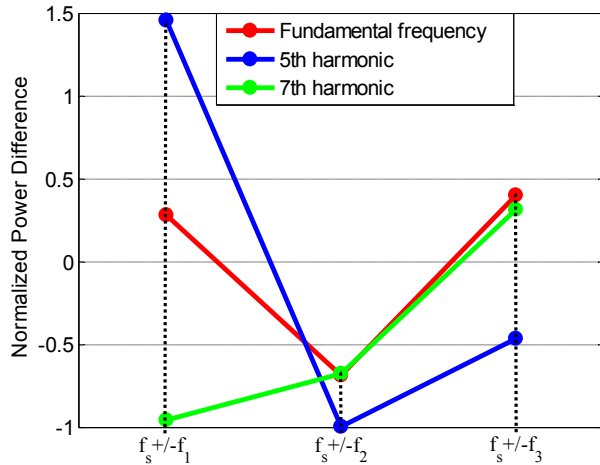Fig. 11. Frequency spectrum obtained from the proposed method.

Fig. 12. Comparison of NPDs at 2% load and variable-speed condition.

VI. CONCLUSION

A mathematical model has been developed to derive the characteristic frequencies in generator stator current measurements for a WT gearbox with gear tooth breaks. An adaptive signal resampling algorithm has been proposed to convert the nonstationary characteristic frequencies to corresponding stationary values for system operating at variable-speed conditions. A fault detector based on statistical analysis on the stator current signatures has been developed for diagnosis of the gear tooth defects. Experiments have been carried out for a two-stage gearbox under both constant-speed conditions and variable-speed conditions to validate the mathematical analysis and the proposed fault detector. For system operating at variable-speed conditions, the proposed adaptive signal resampling algorithm has successfully convert the variable characteristic frequencies of the gearbox tooth break faults to specific constant values. Results have shown that the characteristic frequencies can be clearly observed in the frequency spectra of the generator stator current signal and gear tooth breaks can be effectively identified by using the proposed fault detector.

REFERENCES

[1] J. Ribrant, "Reliability performance and maintenance-a survey of failures in wind power system," M. S. Thesis, KTH School of Electrical Engineering, Stockholm, Sweden, 2006.

[2] P. J. Tavner, *et al.*, "Reliability analysis for wind turbines," *Wind Energy,* vol. 10, pp. 1-18,2007.

[3] J. Ribrant and L. Bertling, "Survey of failures in wind power systems with focus on Swedish wind power plants during 1997-2005," in *Proc. Power Engineering Society General Meeting 2007,* pp. 1-8.

[4] X. Gong, W. Qiao, and W. Zhou, "Incipient bearing fault detection via wind generator stator current and wavelet filter," in *Proc. 36th Annual Conference of the IEEE Industrial Electronics Society*, 2010, pp. 2615-2620.

[5] W. Zhou, *et al.*, "Bearing condition monitoring methods for electric machines: A general review," in *Proc. 2007 IEEE International Symposium on Diagnostics for Electric Machines, Power Electronics and Drives, 2.*, pp. 3-6.

[6] X. Gong and W. Qiao, "Bearing fault detection for direct-drive wind turbines via stator current spectrum analysis," in *Proc. 2011 IEEE Energy Conversion Congress and Exposition*, pp. 313-318.

[7] S.H. Kia, *et al.*, "A modeling approach for gearbox monitoring using stator current signature in induction machines," in *Proc. IEEE Industry Applications Society Annual Meeting 2008*, pp. 1-6.

[8] S.H. Kia, *et al.*, "Gearbox monitoring using induction machine stator current analysis," in *Proc. 2007. IEEE International Symposium on Diagnostics for Electric Machines, Power Electronics and Drives, ,* pp. 149-154.

[9] R.R. Schoen and T.G. Habetler, "Effects of time-varying loads on rotor fault detection in induction machines," *IEEE Trans. Industry Applications,* vol. 31, pp. 900-906, 1995.

[10] R. Yacamini, *et al.*, "Monitoring torsional vibrations of electro-mechanical systems using stator currents," *Journal of Vibration and Acoustics,* vol. 120, pp. 72-79,1998.

[11] X. Gong and W. Qiao, "Imbalance fault detection of direct-drive wind turbines using generator current signals," *IEEE Trans. Energy Conversion,* vol. 27, pp. 900-906, 2012.

[12] M. Feldman, *Hilbert Transform Application in Mechanical Vibration*, 1st ed., Wiley, April 5, 2011.